PREDICTION OF SUBSYNCHRONOUS ROTOR VIBRATION AMPLITUDE CAUSED BY ROTATING STALL

by

Masayuki Kita

Manager, Compressor Designing Section

Hiroshima Turbomachinery Engineering Department

Shinji Iwamoto

Acting Manager, Compressor Designing Section

Hiroshima Turbomachinery Engineering Department

Daisuke Kiuchi

Hiroshima Turbomachinery Engineering Department

and

Rinpei Kawashita

Research Engineer, Vibration & Noise Control Laboratory

Takasago Research & Development Center

Mitsubishi Heavy Industries, Ltd.

Takasago, Japan

Masayuki Kita presently is the Manager of the Compressor Designing Section within the Turbo Machinery Engineering Department, Mitsubishi Heavy Industries, LTD., in Hiroshima, Japan. He is engaged in the design and development of single shaft and integrally geared process centrifugal compressors and expander-compressors for use in petroleum, chemical, and gas industry services that handle air and gas in accordance with API Standard 617.

Mr. Kita received B.S. and M.S. degrees (Mechanical Engineering) from Shizuoka University.

Shinji Iwamoto presently is an Acting Manager of the Compressor Designing Section within the Turbo Machinery Engineering Department, Mitsubishi Heavy Industries, LTD., in Hiroshima, Japan. He is engaged in the design and development of centrifugal compressors for use in petroleum, chemical, and gas industry services that handle air and gas in accordance with API Standard 617.

Mr. Iwamoto received B.S. and M.S. degrees (Mechanical Engineering) from Kyushu University.

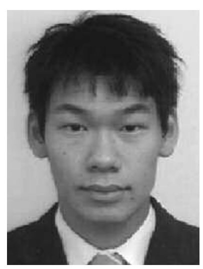

Rinpei Kawashita is a Research Engineer in the Vibration & Noise Control Laboratory in Takasago Research & Development Center, Mitsubishi Heavy Industries, LTD., in Takasago, Japan. He has been a specialist of rotordynamics and engaged in research and development of steam turbines, gas turbines, centrifugal compressors, and other rotating machinery for four years.

Mr. Kawashita received B.S. and M.S. degrees (Mechanical Engineering) from Kyushu University.

ABSTRACT

The prediction of rotating stalls is one of the most important key technologies for compressors, especially high-pressure compressors. The operating ranges of compressors are restricted by rotating stalls because they may cause severe subsynchronous vibration of the rotor. As a consequence, there are many papers that have reported on the subject, including the influence of vaneless diffuser geometry on rotating stalls, and predictions of when a rotating stall occurs through experiment and theory. But, so far, there is no way to predict accurately the amplitude of subsynchronous rotor vibration caused by a rotating stall.

In this paper, the pressure fluctuation caused by rotating stall and the resulting vibration of the rotor were measured using a test rig.

The external force on the impeller during a rotating stall was estimated from the measured pressure fluctuation. The subsynchronous vibration amplitude was then calculated using rotordynamics analysis by adding this external force.

Comparing the result of this rotordynamics analysis with the measured subsynchronous vibration, an influence factor of pressure fluctuation to rotor vibration, β, was calculated. The accuracy of this factor β was checked by comparison with the result of a shop test on a compressor. Using this factor, the subsynchronous rotor vibration level caused by a rotating stall can then be predicted at the design stage.

INTRODUCTION

Many kinds of studies on rotating stalls have been carried out because this phenomenon not only adversely affects the performance of the compressor, but also causes subsynchronous vibration of the compressor rotor, especially with high-pressure services.

The compressor operating range may be restricted by a rotating stall, because it usually occurs prior to a surge. It is usually inevitable that a rotating stall occurs prior to a surge for all designs. But what must be avoided is severe rotor vibration due to a rotating stall, not the rotating stall phenomenon itself.

The purpose of this paper is to establish a method of predicting the subsynchronous rotor vibration level caused by a rotating stall at the design stage of centrifugal compressors.

TEST BY SINGLE IMPELLER TEST RIG

Test Rig Arrangement

The tests were performed in a test rig, the rotor of which has one impeller and was supported by the two ball bearings as shown in Figure 1. The selected design flow coefficient of the impeller is 0.02, because most rotating stall problems occur with low flow coefficient impellers. The test rotor was driven by a motor through a speed increasing gear.

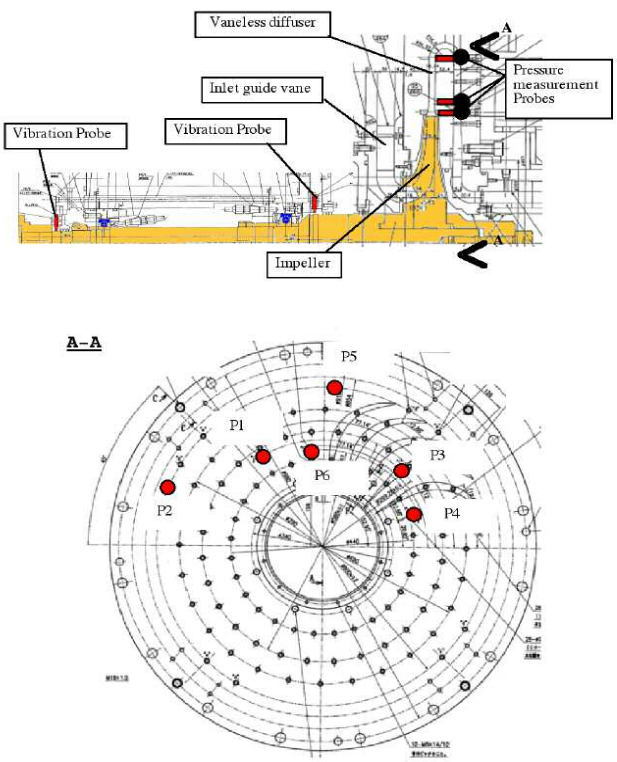

Figure 1. Test Rig Arrangement.

The two vibration probes (horizontal and vertical orientation) were installed as shown in Figure 1. Six pressure measurement probes (P1 through P6) were installed to measure pressure fluctuation at the vaneless diffuser.

The tests were performed by three parameters, which were considered to influence the severity of rotating stall and the flow point at which a rotating stall occurs. The first parameter is diffuser width. From many reports that examined influences of the diffuser width on a rotating stall, the reduction in the diffuser width has a strong influence on the point at which a rotating stall occurs. The ratio of the diffuser width to the impeller outlet width was changed from 0.83 to 0.4.

The second parameter is the clearance of the labyrinth behind the impeller. A rotating stall occurs when the direction of flow reverses locally at the diffuser due to reduction of flow. If the clearance of the labyrinth behind the impeller increases, the flow at the diffuser increases with increased flow. It is thought that this makes the point at which a rotating stall occurs a lower flow level. The clearance of the labyrinth behind the impeller was changed from 0 to .039 inches (0 to 1.0 mm) diameter.

The third parameter is the machine Mach number. In general, it is known that if the machine Mach number increases, the pressure fluctuation caused by a rotating stall becomes larger, as does the point at which the rotating stall occurs. The machine Mach number was changed from 0.3 to 0.7. Test conditions are summarized in Table 1.

Table 1. Summary of Test Conditions.

	Diffuser width /Impeller exit width b4/b2	Labyrinth Clearance behind the impeller (mm)	Machine Mach No. (-)	Run No.	Mark
Case1	0.83	0	0.7	Run1	—●—
			0.5	Run2	—●—
			0.3	Run3	—●—
Case2	0.83	1.0 (Max)	0.7	Run4	—▲—
			0.5	Run5	—▲—
			0.3	Run6	—▲—
Case3	0.6	0	0.7	Run7	—■—
			0.5	Run8	—■—
			0.3	Run9	—■—
Case4	0.6	1.0 (Max)	0.7	Run10	—◆—
			0.5	Run11	—◆—
			0.3	Run12	—◆—
Case5	0.83	0.5 (Nor)	0.7	Run13	—×—
			0.5	Run14	—×—
			0.3	Run15	—×—
Case6	0.4	0	0.7	Run16	—+—
			0.5	Run17	—+—
			0.3	Run18	—+—

Test Results

The six test cases were carried out as shown in Table 1. Figures 2 and 3 show the pressure fluctuation and vibration spectra during the rotating stall in Case 1. By comparing these figures, it was found that there was a correlation between the pressure fluctuation and the rotor vibration at around 15 Hz.

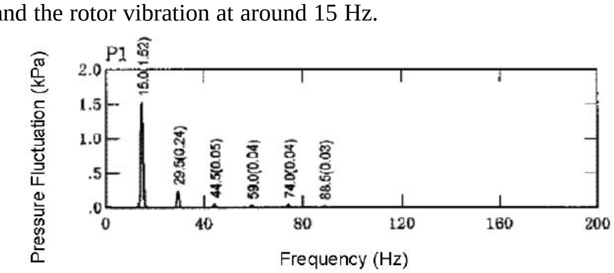

Figure 2. Spectra of Pressure Fluctuation.

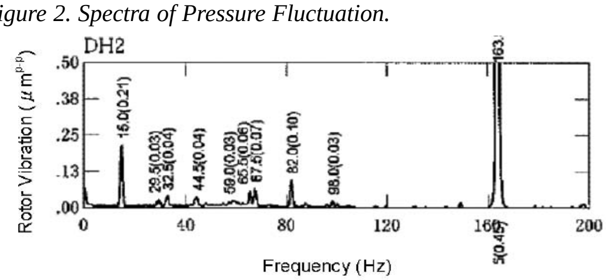

Figure 3. Spectra of Rotor Vibration.

Figure 4 shows the relationship between the pressure fluctuation caused by a rotating stall and the flow coefficient for all cases. Figure 5 shows the relationship between the subsynchronous vibration amplitude and the flow coefficient for all cases. From these results, the followings are found:

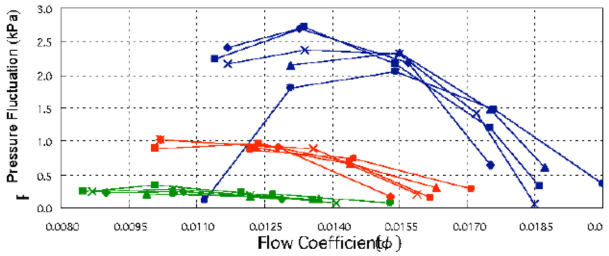

Figure 4. Relationship Between Pressure Fluctuation by Rotating Stall and Flow Coefficient.

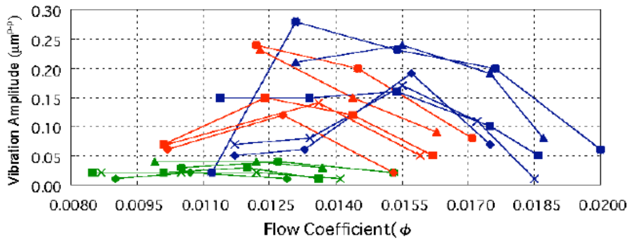

Figure 5. Relationship Between Subsynchronous Vibration Amplitude by Rotating Stall and Flow Coefficient.

- As the flow reduces, the pressure fluctuation increases. However, as it reaches a certain level it does not increase any further.
- As the flow reduces, the number of cells during a rotating stall is increased from two to three. For many cases, as the number of cells increases, the pressure fluctuation and subsynchronous vibration amplitude decreases.
- Figures 4 and 5 show similar patterns of behavior, but in Figure 5, the effects of changing the test parameters are larger.

Figure 6 shows the ratio of the frequency of a rotating stall, f, to the rotational frequency of the rotor, N. From this figure, it is found that the frequency of a rotating stall increases as the flow decreases. Furthermore as the number of cells increases from two to three, the frequency of a rotating stall also increases.

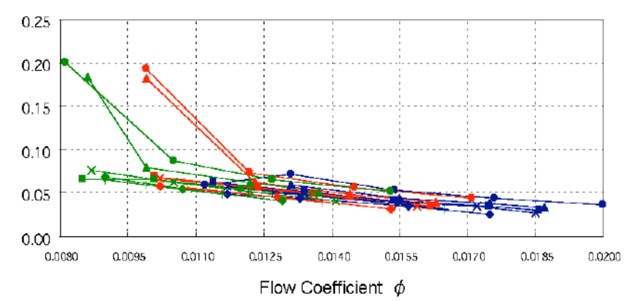

Figure 6. Ratio of Frequency of Rotating Stall to Rotational Frequency of Rotor.

Figure 7 shows the relationship of pressure fluctuation measured by pressure measurement probes P1 and P2 shown in Figure 1. The amplitude of the pressure fluctuation is larger at P1, because the rotating stall occurs near the impeller exit. However, by reducing the flow, the ratio of P2/P1 increases. This means that the region of the pressure fluctuation cell spreads radially as flow reduces.

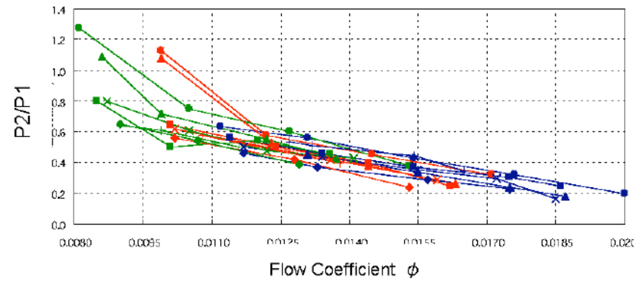

Figure 7. Relationship of Pressure Fluctuation Measured by Pressure Measurement Probe P1 and P2.

PREDICTION OF VIBRATION LEVEL

Prediction by Pressure Fluctuation Level

Assuming the pressure fluctuation magnitude at the diffuser is known, to establish the effect of a rotating stall on subsynchronous rotor vibration level, it should be examined how much the external force from pressure fluctuation affects the rotor vibration. If the influence factor of pressure fluctuation as the external force to the rotor vibration is found, it will be included in the rotordynamics analysis as an external force, and the subsynchronous vibration amplitude caused by the external force can be estimated.

Figure 8 shows the relationship between the pressure fluctuation and the subsynchronous vibration measured with the test rig for Case 1. This figure shows that the vibration amplitude is proportional to the pressure fluctuation. Furthermore, the influence factor of pressure fluctuation to the vibration, α defined by the following equation, can be derived:

$$\alpha = \left(F / S / P_{dout}\right) / \left(P_{AC} / P_{dout}\right) \qquad \textbf{(1)}$$

where,

F = External force
S = Impeller projection area
P_{AC} = Pressure fluctuation at diffuser inlet (impeller outlet)
P_{dout} = Dynamic pressure at diffuser inlet (impeller outlet)

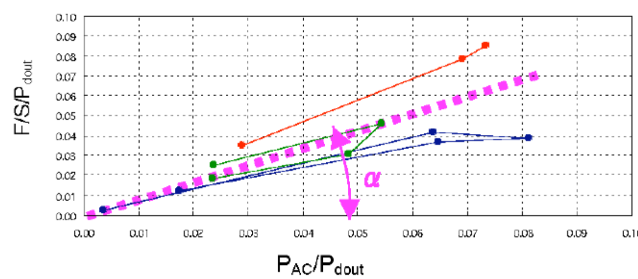

Figure 8. Relationship Between Pressure Fluctuation and Subsynchronous Vibration (Case 1).

Figure 9 summarizes this factor α for all cases. The factor varies with the test conditions, but the maximum value is approximately 0.6.

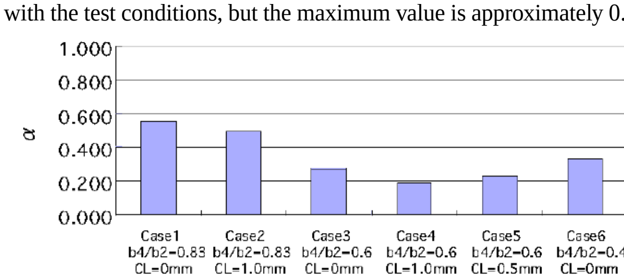

Figure 9. Summary of Factor α for all Cases.

Prediction by Dynamic Pressure Difference

In order to know the pressure fluctuation level during a rotating stall, a computational fluid dynamics (CFD) analysis or experimental study is necessary. However, this would require enormous time and cost. Therefore a more efficient way to predict the subsynchronous vibration level was proposed. As an alternative of α, the external force was derived from the difference in the dynamic pressures between the impeller inlet and outlet at the design stage.

Figure 10 shows the relationship between the difference of the dynamic pressures and the subsynchronous vibration measured with the test rig for Case 1. Applying the same concept as α, by introducing β defined by the following equation, the influence of the pressure fluctuation on the vibration can be estimated.

$$\beta = (F / S) / \Delta P \qquad \textbf{(2)}$$

where,

ΔP = Difference of dynamic pressures between inlet and outlet of impeller

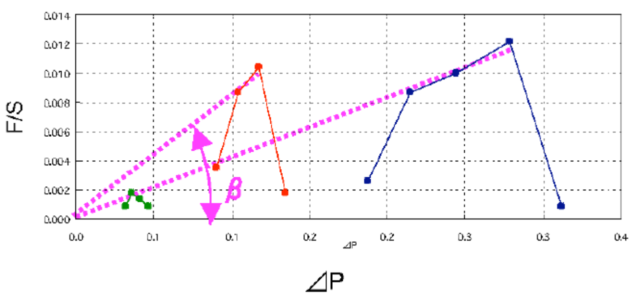

Figure 10. Relationship Between Difference of Dynamic Pressure and Subsynchronous Vibration (Case 1).

Figure 11 summarizes this factor β for all cases. Although the factor varies with test conditions, the maximum value is approximately 0.06.

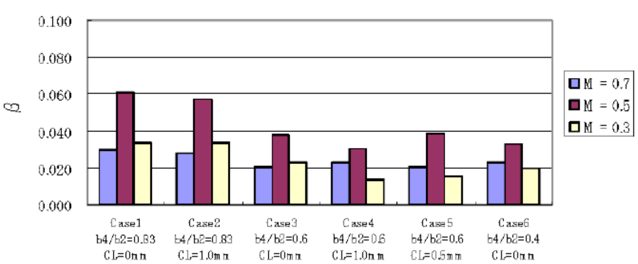

Figure 11. Summary of factor β for all Cases.

COMPARISON WITH SHOP TEST RESULT OF AN ACTUAL MACHINE

In order to confirm the validity of factor β, the pressure fluctuation and subsynchronous vibration were measured using an actual compressor. By the same procedure, the influence factor of β was derived. The result was compared with the factor β derived from the single impeller test results.

Test Arrangement

The shop tests were performed using a back-to-back type compressor, which has four impellers in the low-pressure section and three impellers in the high-pressure section. The impeller flow coefficients were approximately 0.008 to 0.024. The test was carried out under the condition of partial-load around 350 kW. During the test, rotor vibrations were measured using two vibration probes for each end (drive and nondrive end). At the same time, the pressure fluctuations were measured at the exit of the discharge scrolls for each section. The test arrangement is shown in Figure 12.

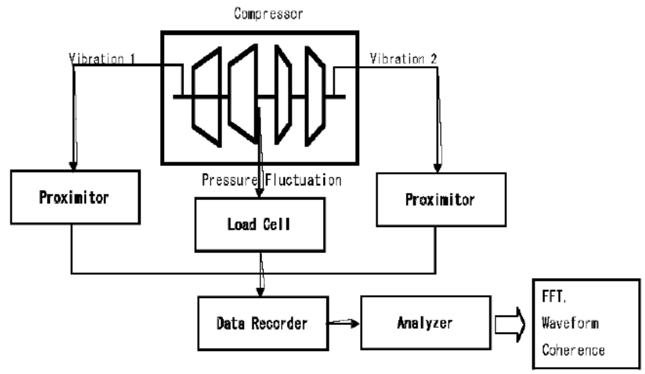

Figure 12. Block Diagram for Measurement.

Test Results

Figure 13 shows the performance curve for the low-pressure section of the compressor under test conditions. During the test, a rotating stall was observed at the measured test points #341 and #351.

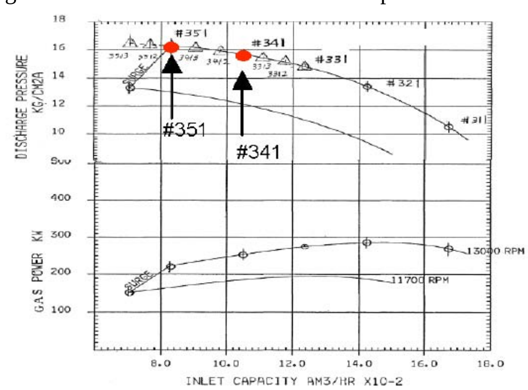

Figure 13. Performance Curve of Test Condition.

Figures 14 and 15 show 3D spectra diagrams of the pressure fluctuation and the rotor vibration measured at test point #351. At this point, pressure fluctuations were observed at frequencies around 11.7 Hz and 23.4 Hz. These frequencies were considered to be caused by a rotating stall. At the same time as this pressure fluctuation, the vibration amplitude of the same frequencies was increased.

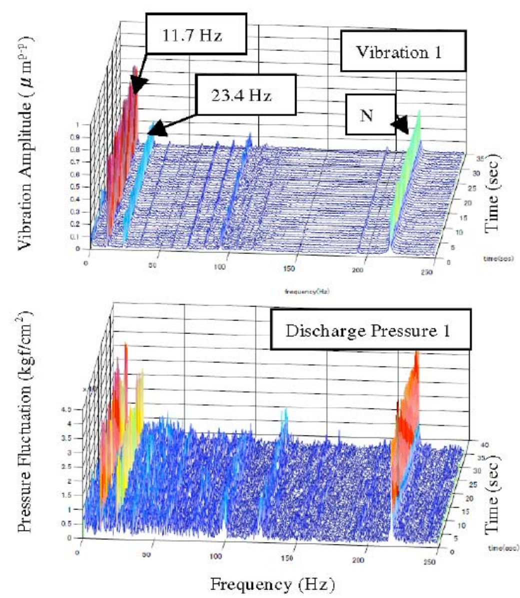

Figure 14. 3D Spectra of Rotor Vibration and Pressure Fluctuation for Low-Pressure Section.

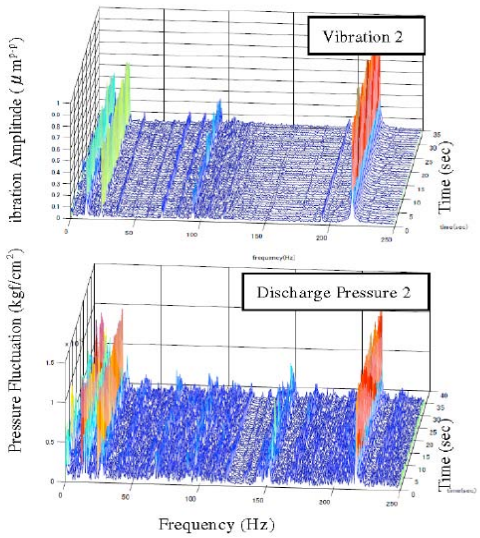

Figure 15. 3D Spectra of Rotor Vibration and Pressure Fluctuation for High-Pressure Section.

Figures 16 and 17 show coherence between pressure fluctuation and rotor vibration. From these figures, there was a clear correlation between pressure fluctuation and rotor vibration at frequencies of 11.7 Hz and 23.4 Hz in addition to synchronous frequency.

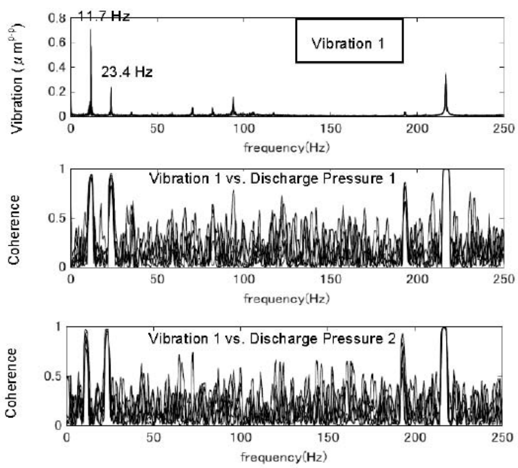

Figure 16. Coherence Between Pressure Fluctuation and Rotor Vibration (Vibration-1).

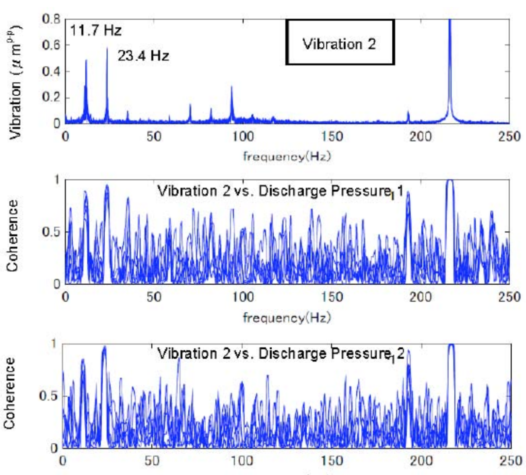

Figure 17. Coherence Between Pressure Fluctuation and Rotor Vibration (Vibration-2).

In particular, at the frequency of 11.7 Hz, there was a strong correlation between rotor vibration-1 and pressure fluctuation-1. And at the frequency of 23.4 Hz, there was a strong correlation between rotor vibration-2 and pressure fluctuation-2. From these results, it was concluded that the frequency of a rotating stall for the low-pressure section was 11.7 Hz, and the frequency of a rotating stall for the high-pressure section was 23.4 Hz.

Figure 18 shows the waveform of the pressure fluctuation level and the rotor vibration level. In order to compare each level at the frequency of a rotating stall, a band pass filter for 11.7 Hz was used. From these figures, one can see that the pressure fluctuation and the rotor vibration level tend to vary in the same fashion.

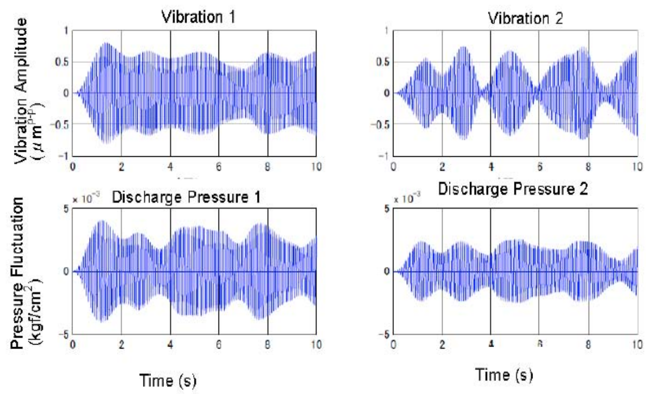

Figure 18. Time Dependence Waveform of Pressure Fluctuation and Rotor Vibration.

VIBRATION ANALYSIS BY ROTORDYNAMICS

Figure 19 shows the model of the compressor rotor for rotordynamics analysis. For the analysis, the maximum, normal, and minimum bearing coefficients were used by considering the bearing lube oil temperature of 118.4°F ± 5°F (48°C ± 5°C) and manufacturing tolerance of bearing clearance (Cp).

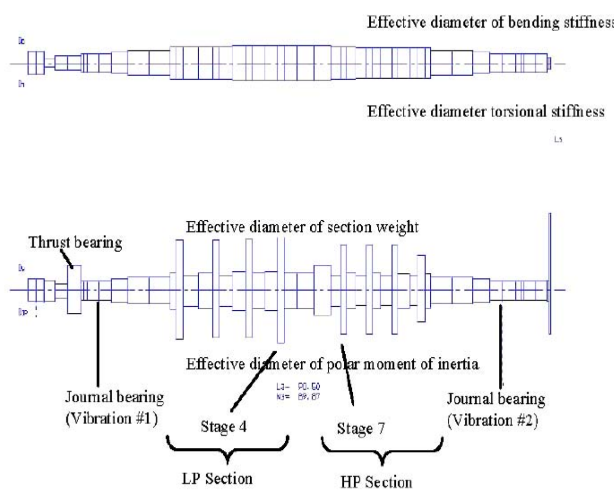

Figure 19. Compressor Rotor Model.

The rotating stall was expected to occur at the last impeller stage of each section. Therefore, the unit external force from the rotating stall was added on the impeller of Stage 4 or Stage 7. The results of the analysis are shown in Figure 20. From these results, the subsynchronous vibration level from a unit force of a rotating stall was estimated.

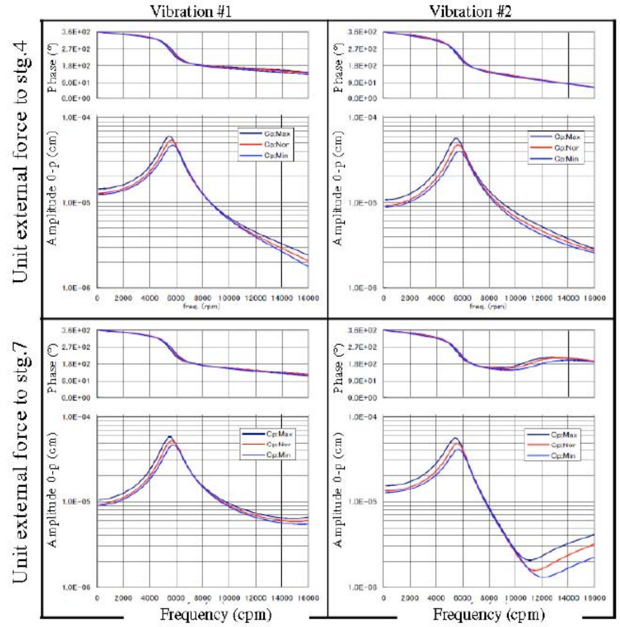

Figure 20. Result of Rotordynamics Analysis.

The vibration amplitude in Figure 20 was calculated using the unit force. In this way, the expected subsynchronous vibration amplitude could be calculated using the vibration amplitude at 11.7 Hz or 23.4 Hz in Figure 20 multiplied by F. By comparing the expected subsynchronous vibration amplitude with the measured vibration amplitude at the shop test, the factor β could be obtained.

Figure 21 shows the summary of the factor, β, obtained by the above procedure. The resultant β was approximately 0.15.

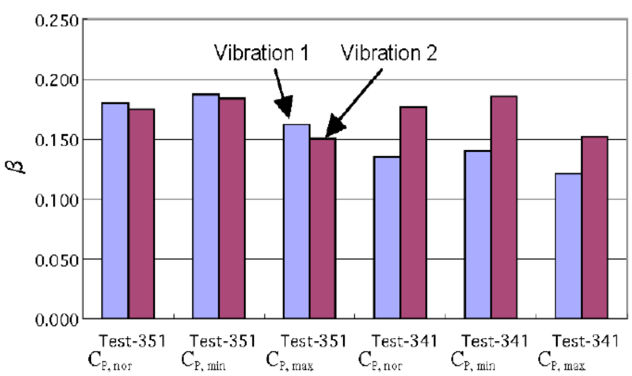

Figure 21. Summary of Factor β for Each Bearing Coefficient at Point #341 and #351.

There was a difference between β of 0.06 obtained from the single impeller test and β of 0.15 obtained from the shop test. The reasons for this difference might be explained as follows:

1. Rotating stall may occur in the stages other than the last impeller and the induced external force may be larger than the assumption in this study.

2. The estimated increment of dynamic pressure from inlet to outlet of the last impellers was smaller than the actual one.

At the design stage, β should be considered as more than 0.15 in order to judge on the safe side. As the proposed value, β of 0.20 should be used. The accuracy of β should be improved by many future shop tests.

CONCLUSION

The effect of the pressure fluctuation from a rotating stall on the rotor subsynchronous vibration was investigated. The pressure fluctuation level and the subsynchronous level were measured with a single impeller test rig, and also by using an actual compressor.

Using these test results and the rotordynamics analysis, the influence factor β was estimated as the factor that shows how much pressure fluctuation works as an external force on the rotor. The estimated β was approximately 0.15. β of 0.20 was proposed in order to be on the safe side during the design stage. The accuracy of β should be improved by many future shop tests.

BIBLIOGRAPHY

Ferrara, G., Ferrari, L., and Baldassarre, L, 2006, "Experimental Characterization of Vaneless Diffuser Rotating Stall Part V: Influence of Diffuser Geometry on Stall Inception and Performance (3rd Impeller Tested)," ASME Turbo Expo 2006: Power for Land, Sea and Air, GT2006-90698.

Fulton, J. W. and Blair, W. G., 1995, "Experience with Empirical Criteria for Rotating Stall in Radial Vaneless Diffusers," *Proceedings of the Twenty-Fourth Turbomachinery Symposium*, Turbomachinery Laboratory, Texas A&M University, College Station, Texas, pp. 97-106.

Kushner, F., 1996, "Dynamic Data Analysis of Compressor Rotating Stall," *Proceedings of the Twenty-Fifth Turbomachinery Symposium*, Turbomachinery Laboratory, Texas A&M University, College Station, Texas, pp. 71-81.

Nishida, H., Kobayashi, H., Takagi, T., and Fukushima, Y., 1988, "A Study on the Rotating Stall of Centrifugal Compressors (1st Report, Effect of Vaneless Diffuser Width on Rotating Stall)," Transactions Japan Society of Mechanical Engineers (B Edition), *54*, (449), pp. 589-594.

Nishida, H., Kobayashi, H., Takagi, T., and Fukushima, Y., 1990, "A Study on the Rotating Stall of Centrifugal Compressors (2nd Report, Effect of Vaneless Diffuser Inlet Shape on Rotating Stall)," Transactions Japan Society of Mechanical Engineers (B Edition), *54*, (449), pp. 589-594.

Senoo, Y. and Kinoshita, Y., March 1977, "Influence of Inlet Flow Conditions and Geometries of Centrifugal Vaneless Diffusers on Critical Flow Angle for Reverse Flow," *ASME Journal of Fluids Engineering*, pp. 98-103.

Senoo, Y. and Kinoshita, Y., 1978, "Limits of Rotating Stall and Stall in Vaneless Diffuser of Centrifugal Compressors," ASME Paper No. 78-GT-23.

ACKNOWLEDGEMENT

The authors gratefully wish to acknowledge the following individuals for their contribution and technical assistance in analyzing and reviewing the results, and for their great suggestions and guidance for practical applications and tests: K. Miyagawa, K. Yamashita, J. Masutani, and M. Ishikawa, of Mitsubishi Heavy Industries.